Engineering Structures 30 (2008) 3082–3094

Contents lists available at ScienceDirect

Engineering Structures

journal homepage: www.elsevier.com/locate/engstruct

Identification of localized frame parameters using higher natural modes

Wei-Jian Yi [a,1], Yun Zhou [a,*], S. Kunnath [b,a], Bin Xu [a]

[a] College of Civil Engineering, Hunan University, Changsha, Hunan 410082, PR China

[b] Department of Civil and Environmental Engineering, University of California at Davis, United States

ARTICLE INFO

Article history:
Received 16 January 2007
Received in revised form
4 April 2008
Accepted 6 April 2008
Available online 27 May 2008

Keywords:
Higher modes
Highly sensitive higher modes
PolyMAX method
Damage diagnosis
Structural parameter identification

ABSTRACT

The use of sensitive higher modes in physical structural parameter identification of local members in a frame system is discussed in this paper. Analytical studies are supported by low-level vibration tests on a third-scale four-story reinforced concrete frame structure embedded in soil to represent a realistic foundation system. Preliminary numerical modal analysis are carried out to establish the sensitivity of higher modes to localized damage in the frame. Damage to one of the elements on the first story of the frame was simulated by adding a mass to the column and examining the vibration modes before and after the addition of the mass. Through forced vibration tests and selective placement of strain transducers, the Poly-reference least-squares complex frequency domain method (PolyMAX) is used to determine the existence of 'highly sensitive higher modes' (HSHMs). An evaluation of the identified higher modes further enables the identification of physical parameters of the target column element using a simple minimization scheme. Findings from the present study indicate that physical parameters of a local element in a frame structure can be identified effectively using HSHMs and that the higher modes of vibration are more sensitive to changes in local physical parameters than lower global modes. The identification of physical parameters as outlined in this study can be applied in structural damage detection.

© 2008 Elsevier Ltd. All rights reserved.

1. Introduction

The existence of structural damage in an engineering structure leads to the modification of vibration modes. Dynamic testing is one means of estimating the changes in the modal parameters such as natural frequencies, mode shapes and modal damping. Natural frequencies and mode shapes provide a 'global' way of assessing the state of a structure. Dynamics-based damage identification methods have drawn wide attention due to their efficiency and ease in implementation. In earlier studies, Cawley et al. [1] used eigenvalues to identify physical structural parameters. Salawu [2] reviewed vibration monitoring in structural assessment procedures and various methods proposed for detecting damage using natural frequencies. Sohn et al. [3] reviewed structural health monitoring (SHM) techniques and highlighted future research areas necessary to advance the field of SHM. However, one of the problems with damage detection using modal data is the fact that global eigenvalues and mode shapes are usually insensitive to the local damage. The local variation in dynamic characteristics cannot be identified exactly using global natural frequencies and mode shapes, especially for large-scale structures.

Higher modes (HMs) in large frame structural systems are more localized than lower modes (LMs) since HMs often represent local member vibration characteristics. Mode localization is a dynamic phenomenon associated with weakly-coupled periodic structures, and results from small imperfections which perturb the periodicity. Hence, HMs are generally more significant in identifying local structural damage. Local modes of a dynamic system have been used for local parameter identification, for example, measured vibration frequencies of cables in a cable-stayed bridge can be used to evaluate tension forces in the cables.

Many researchers have studied higher local modes in engineering structures. Pierre et al. [4] employed a perturbation method to obtain local vibration characteristics without global dynamic analysis of a non-equal span continuous beam. Bendiksen et al. [5] showed that the disorder of modes can lead to local acute changes and found that the localization concentrates in large-scale weakly coupled structure. Cornwell et al. [6] studied mode localization phenomenon on a spatial reflector. Levne-West et al. [7] tested a full-scale 12-rib loosely-coupled antenna for various levels of inter-rib coupling stiffness and excitation force, and validated the mode localization phenomenon for space structures. Bouzit et al. [8] conducted experiments on a nominally periodic twelve-span beam with equal spacing and corresponding disordered beam with

* Corresponding author.
E-mail addresses: hunuyi2006@gmail.com (W.-J. Yi), zhouyun05@126.com (Y. Zhou), skkunnath@ucdavis.edu (S. Kunnath), binxu@hnu.cn (B. Xu).
[1] Tel.: +86 0731 8821532.

0141-0296/$ – see front matter © 2008 Elsevier Ltd. All rights reserved.
doi:10.1016/j.engstruct.2008.04.012

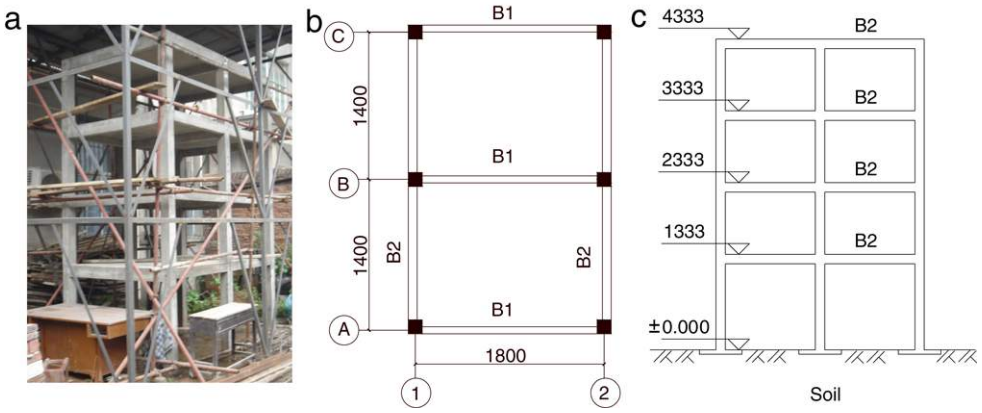

Fig. 1. Frame Configuration; (a) Photo of the model frame structure; (b) Plan view and dimensions; (c) Elevation of North–South frames (all dimensions are in mm).

randomly spaced supports, and demonstrated that the transmission of vibration which takes place within the passband frequency of the periodic beam is greatly hindered when span length randomness is introduced. Mester et al. [9] examined the effects of imperfections on mode shapes and overall response of a simple "near"-periodic structure. Cox et al. [10] constructed a space antenna, determined its modal properties for various levels of both mistuning and inter-structure coupling, and evaluated the probability and severity of system localization from information on the system substructure imperfections. Shen et al. [11] indicated that modal localization phenomenon usually exists in periodic or cycled symmetrical structures, such as large spatial trusses, continuous beams and communicating antennas. Defects in an ideal periodic structure will destroy the periodicity of the structure and may easily lead to modal localization. Xu [12] utilized the maximum dynamic energy principle to identify local damage and parameters in a frame structure. Qi et al. [13] compared global and local vibrations of a steel bridge with different degree of damage and proved that HM is sensitive to local damage.

Mode localization and its identification, which are seldom utilized and reported in civil engineering applications, constitute the focus of this study. This phenomenon will be measured and evaluated in a frame structure in this paper. Stable sinusoidal sweep and hammer-impact excitation will be used to excite local vibrations of a column in a four story reinforced concrete frame structure with independent footings on the soft soil. The Poly-reference least-squares complex frequency domain method (PolyMAX) will be used to identify modal parameters and highly sensitive higher modes (HSHM) including local and global vibration mode shapes will be analyzed. The Euler beam model with both ends constrained will comprise the numerical model of the column and local vibration modes will be used to identify its physical parameters. Results from the study show that HMs posses localized characteristics while LMs represent the global dynamic properties of the entire frame, and that HMs can be used to identify changes in the physical parameters of the local elements in the frame. The ability to detect such parametric changes has the potential to be applied in damage detection of structures.

2. Modal localization phenomenon in frame structures

2.1. Description of the experimental model

The experiment was carried out on the soil pit in the Structural Engineering laboratory at Hunan University in PR China. The structural model shown in Fig. 1 is a four-story reinforced concrete frame. Beneath each column is an independent embedded foundation with a plan dimension of 0.6 m × 0.6 m. Reinforcement

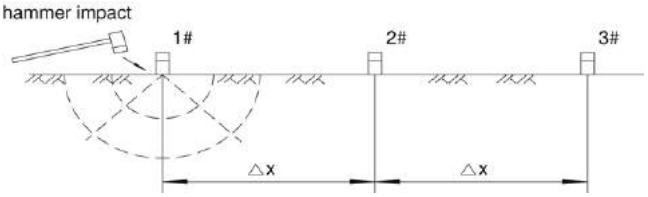

Fig. 2. Rayleigh wave measurement by hammer impact method.

Table 1
Reinforcement data of frame elements

Description	Dimensions (mm)	Reinforcement	
		Longitudinal	Transverse
Columns	133×133	4–Φ 8	Φ3@30 mm
Beams B1	67×167	3–Φ 8 top 3–Φ 8 bot	Φ3@30 mm
Beams B2	83×133	3–Φ 8 bot 2–Φ 8 bot	Φ3@30 mm

details of the beam and column elements are given in Table 1. The floor slab is 30 mm thick and is reinforced nominally with 3 mm diameter bars at a spacing of 30 mm in each direction for both positive and negative bending as needed. The designed yield strength of the reinforcing bars is 235 MPa. The excavated depth of the soil is 1.20 m and beneath this lays undisturbed soil. The pit was filled with clay soil which was compacted at 20–30 cm intervals. The density of the clay is 1965.2 kg/m^3 with a moisture content of 18.85%. Bearing plate experiments indicate that the static elastic modulus of the filled powder clay is 48.1 MPa. A three dimensional soil pressure system TSZ-30B (which is a strain-controlled three-axis pressure system) is used to measure the shear strength of the soil. Based on recorded measurements of four soil samples under different uniform confined pressures, the characteristics of the soil are: $C = 55.8$ kPa and $\varphi = 8.5^\circ$ based on the Mohr–Coulomb criterion.

The dynamic characteristics of the foundation are measured by the impulse excitation method [14]. Three vertical accelerometers are placed 3 m apart in the direction of the transmitting wave as shown in Fig. 2 The hammer used can excite a wide-band frequency response in the soil and transducers are employed to intercept the Rayleigh waves. If the frequency of the Rayleigh wave is f_R, the time difference for the wave to reach adjacent transducers is Δt and the phase difference is $\Delta\varphi$, the transmitting velocity of the Rayleigh wave v_R is defined as

$$v_R = \Delta x/\Delta t = 2\pi f_R \cdot \Delta x/\Delta\varphi. \quad (1)$$

According to elastic wave theory, the relationship between the shear wave velocity v_S and the Rayleigh wave velocity v_R can be

Table 2
Dynamic properties of soil-foundation system

Property	Value
Rayleigh wave velocity v_R	145.54 m/s
Shear wave velocity v_s	156.88 m/s
Dynamic shear modulus G_d	4.837e^7 N/m^2
Dynamic elastic modulus E_d	1.258e^8 N/m

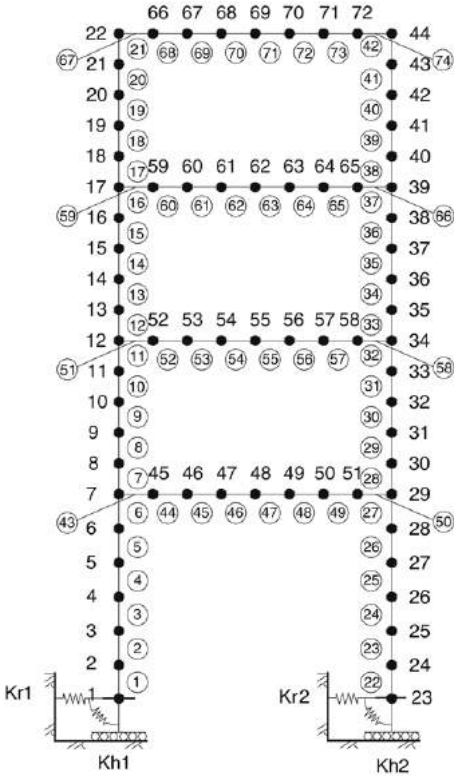

Fig. 3. Numerical model of the frame structure.

written as follows:

$$v_s = \frac{1+v}{0.87+1.12v} \cdot v_R. \tag{2}$$

The dynamic shear modulus G_d and dynamic elastic modulus E_d of the soil are defined as:

$$G_d = \rho v_s^2 \tag{3}$$

$$E_d = 2(1+v)\rho v_s^2 \tag{4}$$

ρ is the density of the soil and v is the damping ratio of the soil. Assuming a damping ratio $v = 0.3$, the soil characteristics shown in Table 2 can be obtained. The elastic modulus of concrete E_c is evaluated in accordance with the empirical expression given in the Chinese Code for Design of Concrete Structures:

$$E_c = \frac{100}{2.2 + 34.7/\bar{f}_{cu}}. \tag{5}$$

In the above expression, $\bar{f}_{cu}$ is the compressive strength obtained from testing of 150 mm cubes. The computed elastic modulus are 32.65, 31.48, 31.99 and 28.57 GPa, for the first through the fourth story levels, respectively.

2.2. Numerical model of the frame

A simplified analytical model of the reinforced concrete frame structure is developed as displayed in Fig. 3. The mass of each slab is concentrated at the corresponding floor beam. In order to account for the effect of the floor slabs, the flexural stiffness of the edge and interior beams are modified to 1.5 E_cI_b and 2 E_cI_b, respectively, as recommended in the Chinese Code. Here E_c is the elastic modulus of concrete and I_b is the moment of inertia of one beam. Therefore, the flexural stiffness of the beams and columns in the planar frame is 5 E_cI_b and 3 E_cI_c respectively, in which I_c is the moment of inertia of one column. The numerical model of the frame structure consists of 74 beam elements.

The dynamic impedance function proposed by Pais et al. [15] is used in the analytical model of the embedded foundation slab. Generally the dynamic impedance function of the foundation is a function of frequency and can be expressed by $a_0 = \omega B/V_s$. The horizontal, rocking, and coupled horizontal-rocking impedance functions are as follows:

$$K_{Hx}^d = K_{Hx}^s(G, B, v, L, e)(1.0 + ia_0c) \tag{6}$$

$$K_{Rx}^d = K_{Rx}^s(G, B, v, L, e, a_0)(k + ia_0c) \tag{7}$$

$$\bar{K}_{HR}^d = (e/B)\bar{K}_{Hx}^d/3 \tag{8}$$

where K^s is defined as the static stiffness of the foundation, ω is natural circular frequency, L and B denote half of the length and width of the foundation, respectively. G is the dynamic shear modulus of the soil, e is the embedded depth of the slab, V_s is the shear wave velocity, and k and c are the dynamic stiffness and damping coefficients of the foundation, respectively.

2.3. Numerical modal analysis

In experimental modal analysis of a regular frame model with concentrated masses at each story, the lower modes (LMs) normally correspond to the global vibration modes of the structure, with the maximum number of modes being equal to the number of stories in the structure. Hence, for the four-story frame structure in this research, only those vibration modes higher than the first four and natural frequencies lower than 500 Hz are considered since one of the main objectives of the study is to find higher modes (HMs) that are sensitive to minor changes in localized physical parameters at the member level rather than at the global structure level. In this investigation, a column in the first story is treated as the target member to be identified by the use of higher modes.

An examination of the basic dynamic equation of equilibrium and the resulting eigenvalue problem reveals that the dynamic properties of a structure are primarily a function of the mass and stiffness, and that changes to these parameters alter the dynamic characteristics of the system. In preparing to develop an experimental program to examine the effects of these primary structural parameters (viz. mass and stiffness), a numerical study is first undertaken. With reference to the frame model shown in Fig. 3, changes to the local properties of the first floor column comprising elements 1 through 6 are considered for the following seven cases: (1) undamaged state of the structure; (2) a 20% stiffness reduction in element 5; (3) a 40% stiffness reduction in element 5; (4) a 60% stiffness reduction in element 5; (5) a 50% increase in the mass of element 5; (6) a 100% increase in the mass of element 5; and (7) a 150% increase in the mass of element 5.

Results from the numerical eigenvalue analysis corresponding to the seven cases are presented in Table 3. It is seen that the natural frequencies of the first four global modes are not sensitive to local damage (or local variations in mass and stiffness), whereas the natural frequencies of the 5th and 6th mode show a perceptible change in vibration properties. In order to compare the mode shapes resulting from stiffness and mass variations introduced in Case (2)–(7) with respect to the original frame of Case (1), the corresponding Modal Assurance Criterion (MAC) values are determined and shown in Table 4. Changes to the 5th and 6th mode

Table 3
Comparison of natural frequencies (Hz) for three cases

Mode →	1st	2nd	3rd	4th	5th	6th	7th	8th	9th	10th	11th
Case 1	8.72	31.07	55.95	78.97	**238.86**	**249.09**	397.21	412.61	416.84	440.15	455.81
Case 2	8.68	31.03	55.92	78.96	**238.51**	**248.80**	397.21	412.57	416.8	440.12	455.66
Case 3	8.62	30.96	55.88	78.96	**237.92**	**248.36**	397.21	412.51	416.74	440.08	455.41
Case 4	8.52	30.85	55.82	78.94	**236.67**	**247.66**	397.20	412.41	416.64	440.00	454.99
Case 5	8.72	30.98	55.82	78.90	**234.76**	**247.31**	397.21	412.56	416.84	440.14	455.53
Case 6	8.71	30.90	55.69	78.83	**230.04**	**246.48**	397.21	412.51	416.83	440.14	455.21
Case 7	8.70	30.81	55.57	78.77	**225.26**	**246.04**	397.21	412.45	416.83	440.13	454.83

Table 4
Comparison of MAC value for different cases

Mode number →	1st	2nd	3rd	4th	5th	6th	7th	8th	9th	10th	11th
MAC(Case1:Case2)	1.0000	1.0000	1.0000	1.0000	**1.0000**	**1.0000**	1.0000	0.9999	0.9999	1.0000	0.9999
MAC(Case1:Case3)	1.0000	0.9999	0.9999	1.0000	**0.9997**	**0.9997**	1.0000	0.9992	0.9993	0.9998	0.9993
MAC(Case1:Case4)	0.9999	0.9998	0.9997	0.9998	**0.9989**	**0.9984**	0.9999	0.9966	0.9969	0.9993	0.9968
MAC(Case1:Case5)	1.0000	1.0000	0.9999	1.0000	**0.9982**	**0.9950**	1.0000	0.9999	1.0000	1.0000	0.9995
MAC(Case1:Case6)	1.0000	0.9999	0.9997	0.9998	**0.9955**	**0.9793**	1.0000	0.9996	0.9999	0.9999	0.9976
MAC(Case1:Case7)	1.0000	0.9998	0.9993	0.9996	**0.9925**	**0.9555**	1.0000	0.9991	0.9999	0.9999	0.9938

Table 5
Comparison of DI value

Frequency order	1st	2nd	3rd	4th	5th	6th	7th	8th	9th	10th	11th
Case 1	0.457	1.226	2.141	2.156	**45.028**	**14.977**	0.026	0.091	0.071	0.051	0.137
Case 2	0.458	1.226	2.134	2.145	**42.239**	**14.636**	0.026	0.093	0.072	0.053	0.141
Case 3	0.459	1.226	2.123	2.130	**38.792**	**14.099**	0.027	0.097	0.074	0.056	0.147
Case 4	0.461	1.226	2.107	2.107	**34.489**	**13.121**	0.029	0.103	0.078	0.061	0.158
Case 5	0.457	1.234	2.150	2.156	**30.340**	**11.744**	0.026	0.103	0.074	0.054	0.165
Case 6	0.458	1.241	2.160	2.155	**25.527**	**9.542**	0.027	0.115	0.077	0.059	0.198
Case 7	0.458	1.248	2.169	2.154	**22.954**	**8.096**	0.027	0.128	0.080	0.064	0.237

Table 6
Comparison of Δ DI value

Frequency order	1st	2nd	3rd	4th	5th	6th	7th	8th	9th	10th	11th
ΔDI_2 (Case1–Case3)	0.001	0.000	0.007	0.011	**2.788**	**0.341**	0.001	0.002	0.001	0.002	0.004
ΔDI_3 (Case1–Case4)	0.002	0.000	0.018	0.026	**6.235**	**0.878**	0.002	0.006	0.003	0.005	0.010
ΔDI_4 (Case1–Case5)	0.004	0.000	0.034	0.049	**10.539**	**1.856**	0.004	0.012	0.007	0.011	0.022
ΔDI_5 (Case1–Case6)	0.000	0.008	0.010	0.001	**14.687**	**3.234**	0.001	0.012	0.003	0.004	0.028
ΔDI_6 (Case1–Case7)	0.001	0.015	0.019	0.001	**19.501**	**5.435**	0.001	0.024	0.006	0.008	0.061
ΔDI_7 (Case1–Case8)	0.001	0.022	0.028	0.002	**22.074**	**6.882**	0.002	0.037	0.009	0.013	0.100

are marginal but not conclusively perceptible. The mode shapes are normalized by Eq. (9), which requires the amplitude of the mode shape vectors:

$$\sum_{i=1}^{N} \varphi_{ir}^2 = 1 \quad (r = 1 \sim 11). \tag{9}$$

In Eq. (9), i is the index of the modal components, r is the mode shape number, and N is the total number of components. The first 11 modes for Case (1) are demonstrated in Fig. 4, where the amplitude of the mode shapes of the beams is relatively small and therefore not plotted in the figure. The modes of each column of the frame vibrate as a half sine wave. Moreover, the amplitudes of the 5th and 6th mode shapes corresponding to the first story columns are much larger than those of other stories. Since the MAC value is not a reliable measure of identifying modal variations caused by localized changes, a mode shape diagnosing index is defined as follows:

$$DI_i = \frac{|\Phi_{1m,i}|}{(|\Phi_{2m,i}| + |\Phi_{3m,i}| + |\Phi_{4m,i}|)/3} \tag{10}$$

$$\Delta DI = |DI_i - DI_R| \tag{11}$$

$\Phi_{1m,i}$, $\Phi_{2m,i}$, $\Phi_{3m,i}$ and $\Phi_{4m,i}$ are the amplitudes of the mode shapes at the mid nodes of the columns of the ith mode in the first, second, third and fourth story, respectively. DI is a measure of the contribution of the localized mode (in the present experiment this corresponds to the first floor where local properties of column element 5 are modified). Obviously, when DI is large, the local mode will dominate the vibration shape. In Eq. (11), subscript R corresponds to the reference configuration which in this case is the original undamaged structure. Hence ΔDI is a measure of the change in the local vibration mode.

Pierre et al. [4] indicated that mode shape localization occurs when the peak ratio of the amplitude of mode shapes of two spans in a continuous beam is larger than 10. In Table 5, it is observed that the DI value of the 5th and 6th modes have maximum values larger than 10, so it can be inferred that these two modes constitute the localization phenomena in this case. Also, as shown in Table 6, ΔDI s of the 5th and 6th mode shapes corresponding to the first story column show the most significant variations, indicating a change in the state of an element on the first floor of the frame. Moreover, only the 5th and 6th mode shapes are sensitive to the parameter variation of the member while the others are not. Hence in this manner, by identifying the maximum changes in the index ΔDI, it is possible to determine those HMs that are 'most' sensitive to local mass and stiffness changes.

In order to examine other factors which also influence the modal localization phenomenon, three different numerical experiments are carried out: (1) frame with equal story heights of 1.0 m; (2) frame with fixed base and equal story height; and finally,

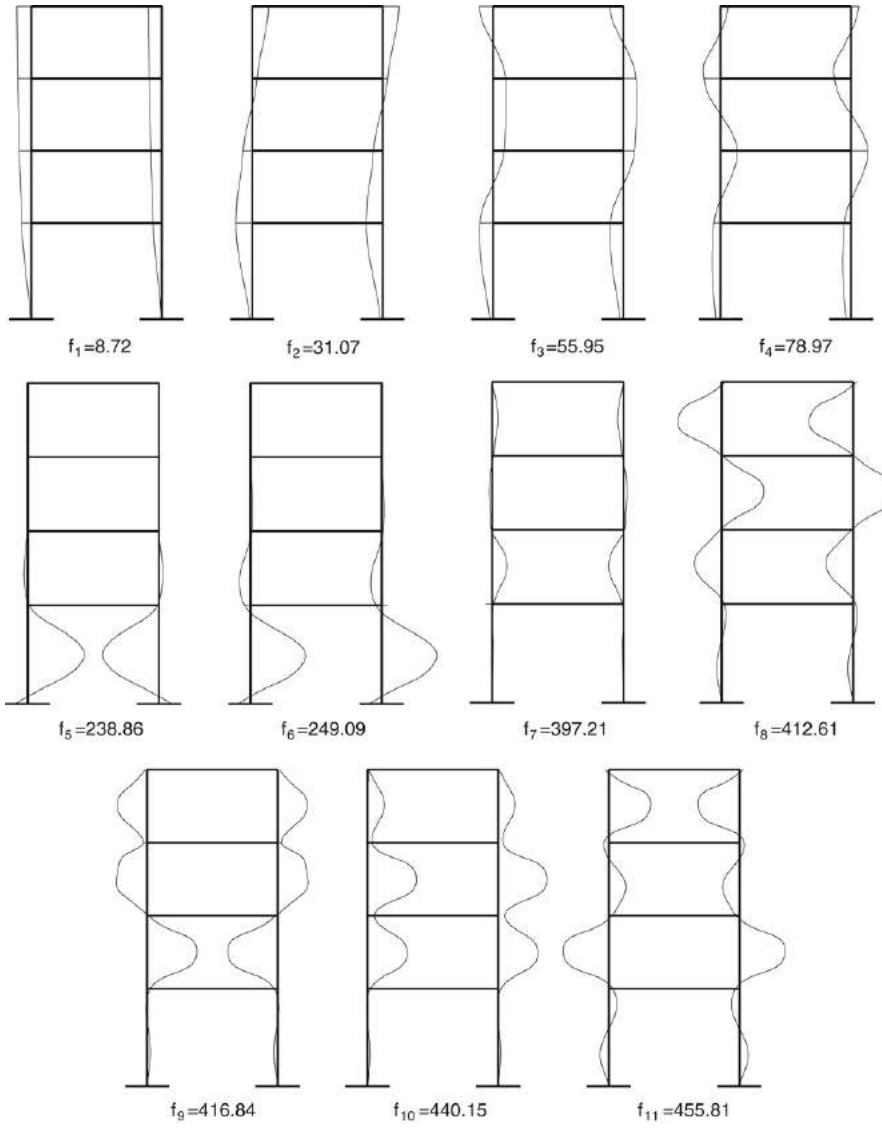

Fig. 4. First 11 mode shapes and frequencies (Hz) of undamaged structure.

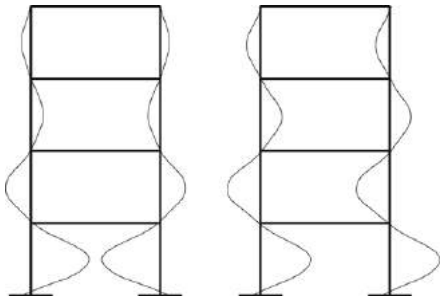

Fig. 5. 5th and 6th vibration mode shapes for regular frame with equal story heights.

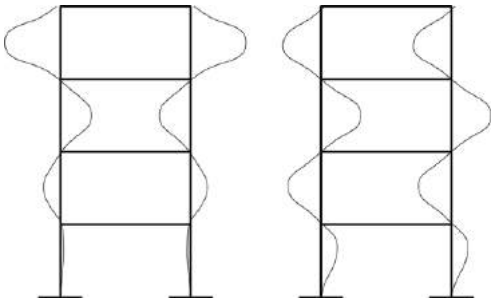

Fig. 6. 5th and 6th vibration mode shapes for fixed base frame with equal story heights.

(3) Fixed-base equal story height frame with elastic modulus of elements 28–32 reduced by 80%. The 5th and 6th mode shapes for these cases are shown in Figs. 5–7. From Fig. 5 it is clear that the mode shape localization phenomenon is weakened when the first story height is equal to that of the other stories, and the *DI* values are reduced to 3–4. In Fig. 6 the amplitudes of the 5th and 6th mode shapes in the first-story are smaller than the remaining stories because the base is fixed and the corresponding *DI* values are smaller than 1. In Fig. 7 it is seen that the column of the frame is similar to an equal span continuous beam, hence when the stiffness of a span (here this corresponds to the column in the second story) is decreased, the modal localization phenomenon occurs in this span. The above numerical simulations show that the dynamic behavior of columns in a frame structure is analogous to a continuous beam. Foundation flexibility and element stiffness are important parameters influencing the localization phenomenon.

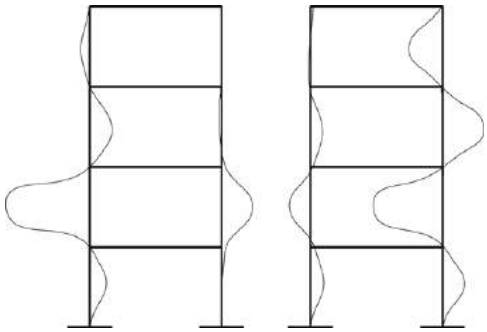

Fig. 7. 5th and 6th vibration mode shapes for fixed base equal story height frame with reduced elastic modulus in elements 28–32.

Fig. 8. Additional mass attached to target column.

From the above numerical modal analyses it is evident that a simple way to detect damage in columns of a frame structure is to determine modes which have relatively large amplitude corresponding to the column to be identified. The natural frequencies and mode shapes of the identified modes should be sensitive to local variations in the properties of the column. The next crucial issue is how to find these modes and whether these modes exist in reality. To investigate these preliminary findings from the numerical study, the following experimental program is designed.

3. Experimental modal testing of frame structure

3.1. Description of experimental procedure

The model shown in Fig. 1 is subjected to a series of non-destructive low impact vibration tests before and after the introduction of localized changes to a column element in the frame. Stiffness degradation in concrete structures due to damage cannot be recovered. In order to investigate the sensitivity of HMs to local property changes, local damage was indirectly simulated in the first-story column of the frame by attaching an additional mass. As shown in Fig. 8, steel plates were attached to the surface of the second element (between point 9 and 10 — see Fig. 9 to identify these locations) of the column. The steel plate measured 0.2 m × 0.2 m × 0.03 m and weighed 9.36 kg, which is equal to the mass of the element. The added mass will decrease the frequency of the element thereby simulating localized damage in the frame.

First, the structure was excited by hammer impact on the middle column of frame axis 2 (see Fig. 1(b) for location) to establish global vibration modes of the base model. A PCB hammer

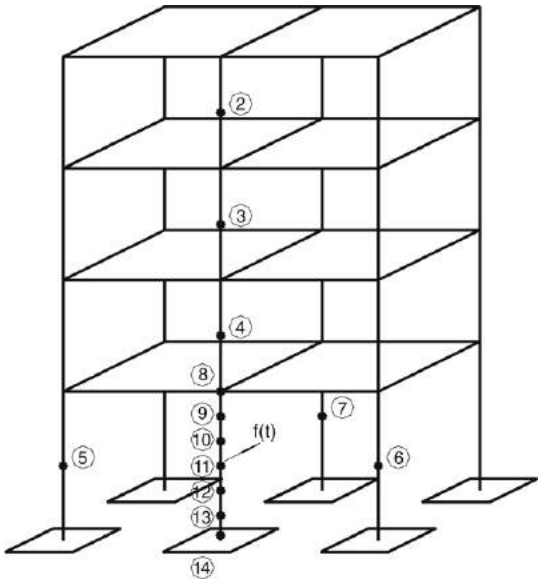

Fig. 9. Harmonic excitation of point 11 at mid height of column and placement of accelerometers.

with a sensitivity of 0.23 mV/N was used to deliver the impact, and numerous accelerometers (sensitivity: 100 mV/g) and an ABACUS signal analyzer (manufactured by Data Physics Corp) were used to collect the vibration signals. The frequency range considered is 0–500 Hz. The upper columns (each 1 m high) are divided into 5 segments, while the lower floor column (1.33 m) is divided into 6 segments. The global modal experiment was carried out across the complete frame height with 22 points on the column and 2 points on the foundation slab.

Next, a higher-order modal test was carried out on the first floor middle column of frame axis (2)-(b) (see Fig. 1(b) for axis location). An electromagnetic oscillator with a maximum exciting force of 500 N was employed to excite the column at point 11 as shown in Figs. 9 and 10 with stable sinusoidal sweeps. The points 2 through 14 are used as the measurement points, and PCB740B02 strain transducers (with sensitivity 52.5 mv/$\mu\varepsilon$) are used to measure modal strains of points 8 through 14. Among the measurement locations, points 2, 3 and 4 are located in the middle of second, third, and fourth story, respectively and these points assist in distinguishing the mode shapes of the upper three stories from that of the first story. Points 5 and 6 are employed to measure the vibrations of axes (A) and (C) to determine whether the three plane frames vibrate in phase and with the same amplitude. This vibration test was carried out at a frequency range 100–500 Hz.

The model frame was excited before and after damage (i.e. added mass) using both the hammer-impact and the electromagnetic oscillator. The PolyMAX method available in LMS TestLab modal analysis software [16] is used to analyze the measured modal parameters. The method first establishes so-called 'stabilization diagrams' to identify the normal modal frequencies, damping and participator factors. The PolyMAX method tries to fit high-order models that contain more vibration modes than present in the data. Next, the true physical modes are separated from spurious numerical ones by interpreting the stabilization diagrams. The poles corresponding to a certain model order are compared to the poles of a one-order-lower model. If the difference is within pre-set limits, the pole is labeled as stable. Spurious numerical poles will not stabilize during this process and can be sorted out of the modal parameter data set [16]. The PolyMAX method provides clear stabilization diagrams and therefore has the advantage of identifying higher damping and higher modes (HMs) in engineering structures. In this study, it is

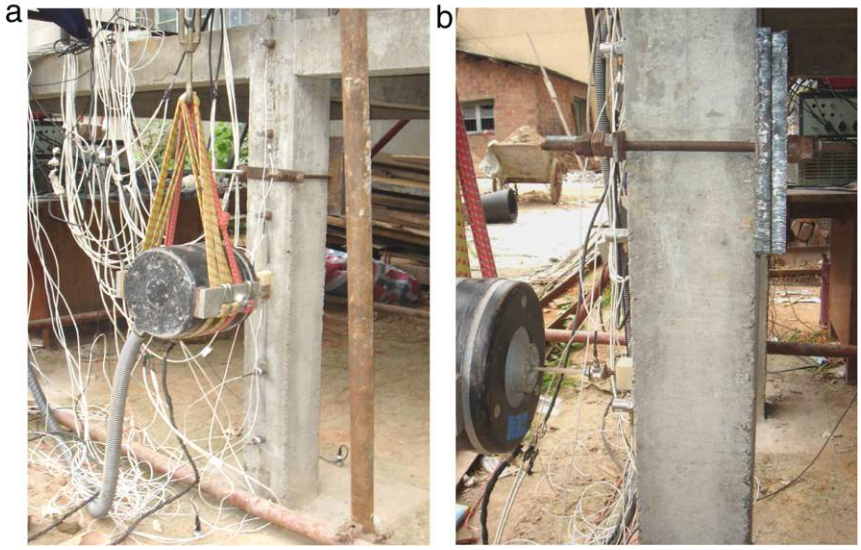

Fig. 10. Modal test by local excitation: (a) Front view; (b) Side view.

Table 7
Comparison of measured first four natural frequencies before and after damage

Natural frequency number	First	Second	Third	Fourth
Natural frequency before damage (Hz)	7.6	25.2	50.2	76.8
Natural frequency after damage (Hz)	7.6	25.1	50.1	76.8
Difference (%)	0	0.397	0.199	0

employed to identify HMs in the range of 100–500 Hz since the first four global modal frequencies of the model frame are lower than 100 Hz.

3.2. Experimental identification of higher modes

The first four measured natural frequencies before and after damage are listed in Table 7 and the corresponding mode shapes are displayed in Fig. 11. The difference between measured (Table 7) and analytically computed (Fig. 4) frequencies can be attributed to the simplifications introduced by aggregating the 3D frame into a planar frame. As expected, there is little or no influence of local damage (or local property variations) on global natural frequencies thus making it impossible to identify local damage using global modes. Next, the stabilization diagrams generated by the PolyMAX method are shown in Figs. 12 and 13. In the stabilization diagram, 'o' denotes that an apex has not been found, 'f' denotes that the frequency is stable (within the tolerance), 'd' indicates that both the frequency and damping ratio are stable and 's' denotes that all three parameters (including pole vector) are stable. As shown in Figs. 12 and 13, higher modes with frequencies larger than 100 Hz concentrate in many regions and in each region there are about three modes. These closely-spaced modes are likely induced by the three planar frames in the measurement direction. Previous studies have shown that eigen-modes of multi-span continuous beams are distributed in different regions called 'passbands'. For the frame structure considered in this study, when the beams and columns vibrate as half sine waves, correlating modes can be found in consecutive passbands. Based on the vibration characteristics of the beams and columns, Regions I–IV belong to the first passband, and Regions beyond V belong to the second passband. In this study, the main focus is on the frequency range lower than 500 Hz; hence higher passbands above 500 Hz are not tested and analyzed.

As indicated previously, a stable sinusoidal sweeping excitation is induced at point 11 using the electromagnetic oscillator and the response signals at points 2–14 are recorded. In order to verify that the three planar frames are vibrating with the same magnitude, the frequency response functions (FRF) of selected locations are examined. Points 11 and 7 are located on two columns of the same plane frame on axis (B). From the FRF of the data recorded at point 11 (shown in Fig. 14), higher modes are located in the fourth region (denoted by 'A') and the corresponding FRF measured at point 7 is denoted by 'B' in the same figure. It is clear that both columns of the frame are excited, and the magnitude of 'A' is larger than that of 'B'. By contrast, as indicated in Fig. 15, the maximum peak of the FRF of point 11 appears in region 'C', and there are no corresponding peaks of the FRF for points 5 and 6 in region 'D', because point 5 and 6 do not lie in the same plane as point 11. Hence it can be concluded that the FRF diagrams do not include the local vibration modes of the adjacent columns.

Measured displacement modes and strain modes of middle column of the frame in the plane of excitation are compared before and after damage. In all, 15 mode shapes were extracted from the experimental measurements in the frequency range 100–500 Hz. The actual number of modes is greater than that obtained in the numerical simulation since the analytical model was simplified by merging the three frames of a 3D structure into a single planar frame. The addition of the mass to the column element results in decreasing the natural frequencies in area IV. Both displacement and strain mode shapes are sensitive to the local damage in the fourth region. A comparison of the frequencies before and after damage is listed in Table 8. In regions I, II, III and V, the frequencies do not have noticeable changes. This indicates that not all of higher modes are sensitive to the changes in local member parameters. The changes in displacement and strain mode shapes for selected higher modes are shown in Figs. 16 and 17. The two mode shapes are measured in two independent experiments. The mass-normalized modes obtained from the LMS software are rescaled using Eq. (9) after normalization — note that the maximum amplitude of the mode shape appears to be the same in the first story though the modal amplitudes are different in the upper three stories. Hence, the *DI* values are calculated and

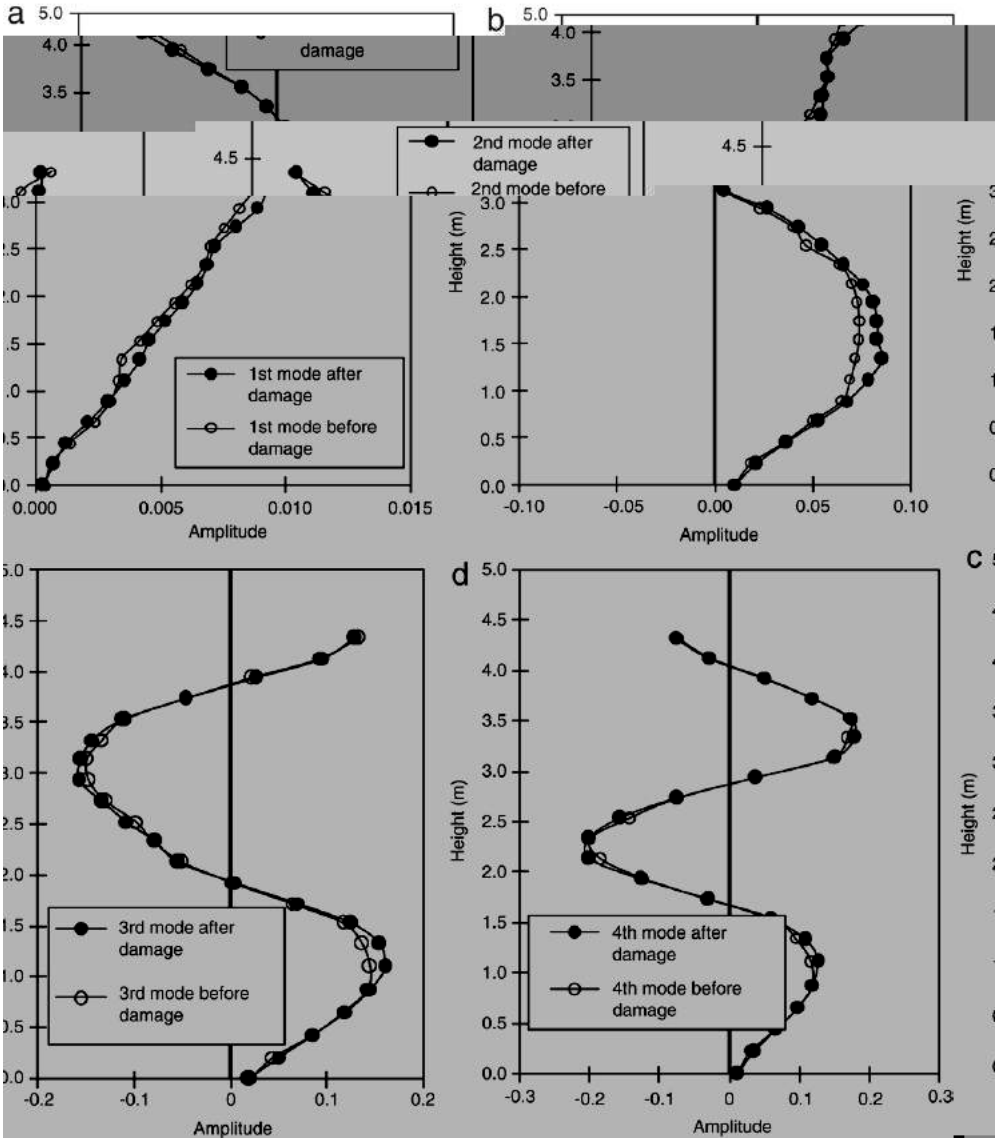

Fig. 11. Comparison global mode shapes before and after damage: (a) – (d): Modes 1–4.

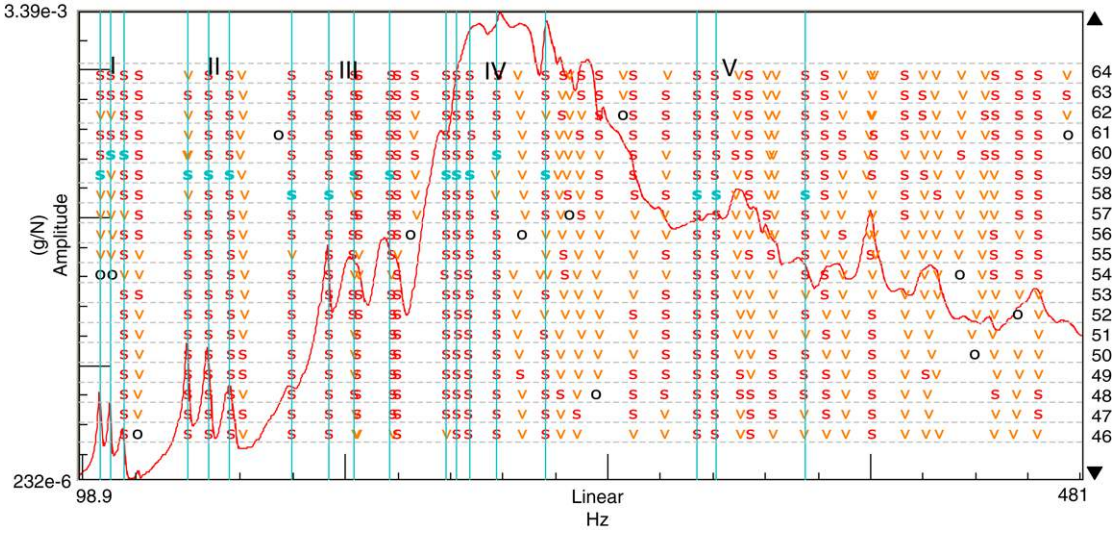

Fig. 12. Stabilization diagram of assembled frequency response function before damage ($g/N = 10\ \mathrm{m/s^2/N}$).

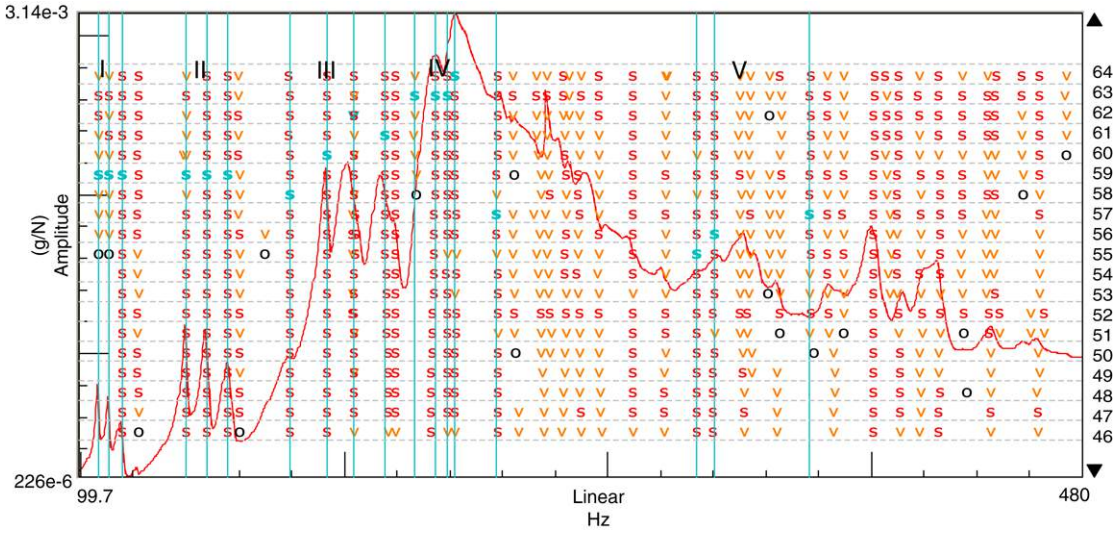

Fig. 13. Stabilization diagram of assembled frequency response function after damage ($g/N = 10\ \mathrm{m/s^2/N}$).

Table 8
Comparison of experimentally measured higher modal frequencies before and after damage

Natural frequency order	5th	6th	7th	8th	9th	10th	11th	12th	13th	14th	15th	16th	17th	18th	19th	/
Before damage (Hz)	106.72	110.82	115.55	139.94	148.02	156.05	193.50	203.20	217.13	247.50	257.34	276.18	333.78	341.05	375.03	/
After damage (Hz)	106.75	110.82	115.52	139.91	147.90	155.88	193.44	203.66	215.40	234.81	238.96	257.91	333.69	340.51	376.70	/
Difference (%)	0.025	0.007	−0.023	−0.026	−0.079	−0.109	−0.030	0.223	−0.795	−5.13	7.143	−6.615	−0.027	−0.158	0.444	/

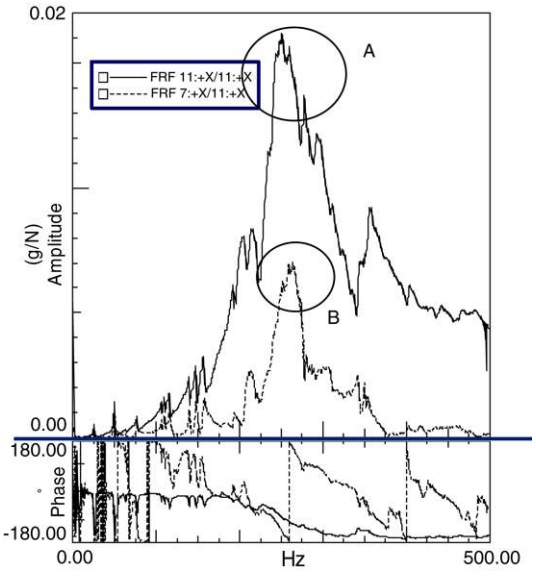

Fig. 14. Comparison of frequency response functions and phase angle between points 11and 7 (Notation: FRF = frequency response function; X: measurement direction; $g/N = 10\ \mathrm{m/s^2/N}$).

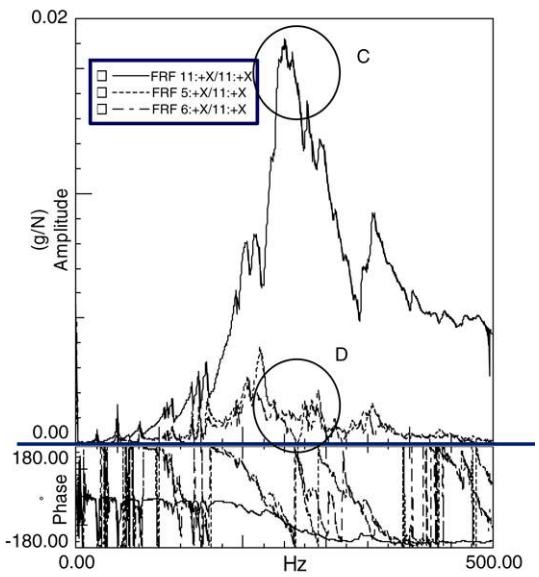

Fig. 15. Comparison of frequency response functions and corresponding phase angles between points 11, 5 and 6.

reported in Table 9. The strain mode shapes (Fig. 17) are also normalized in a similar manner.

From Table 8 it can be seen that the change in 'sensitive' higher modal frequencies (modes 14–16) resulting from the added mass are about 12–18 times the corresponding changes to global lower modal frequencies. Also from Table 9 it is observed that the change in these modes result in a maximum decrease of 29.7% in *DI* value. These modes that are sensitive to local changes are referred to as "highly sensitive higher modes" (HSHMs) and need to be distinguished from other higher modes so that localized damage can be identified through an assessment of the vibration mode shapes. Hence HM frequencies have the potential to be used in damage identification of structures.

Table 9
DI value of 13th–16th measured modal shapes

Mode number	13th	14th	15th	16th
DI (Before damage)	7.61	14.20	2.73	11.90
DI (After damage)	5.58	12.00	2.68	8.36
Change %	26.7	15.5	2	29.7

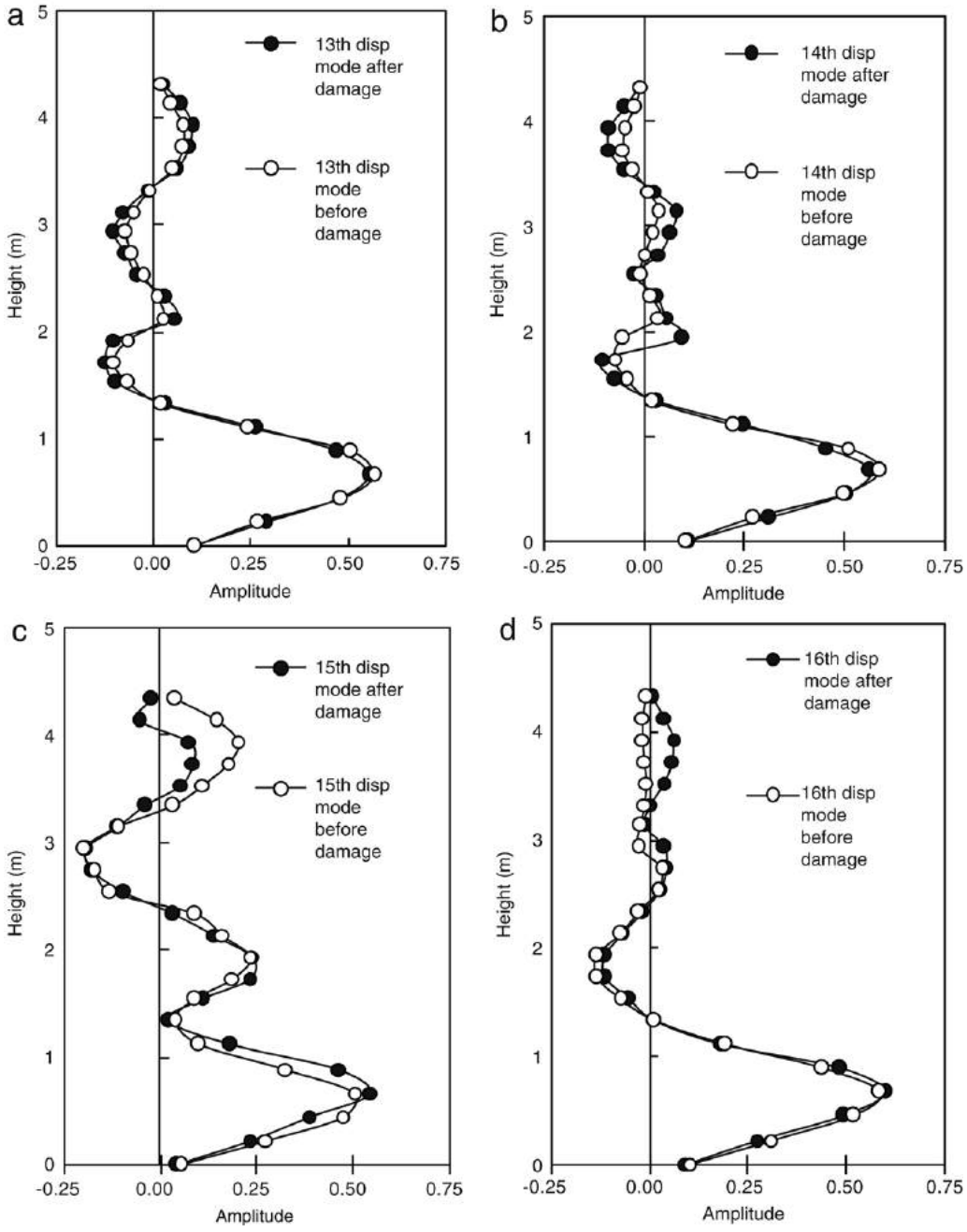

Fig. 16. Changes in displacement mode shapes before and after damage: (a)–(d): 13th–16th mode.

4. Physical parameter identification using higher modes

Modal parameters of the intact (undamaged, i.e. before the mass addition) frame are now used to identify the physical parameter of the local column member. The analytically computed fifth and sixth modes (shown in Fig. 18) with frequencies of 238.86 Hz and 249.09 Hz have the maximum sensitivities. These computed modes match well with measured ones in Region IV and correspond to modes 13 and 14 (see Fig. 16). The 8th–12th modes were not adequately identified in the measurements. The identified 'sensitive' modes will now be used in the identification of physical parameters of the local element.

In the physical parameter identification process, the first-story column of the frame structure is idealized as an Euler beam model with both ends constrained by horizontal and rotational springs as shown in Fig. 19. At the bottom of the column, kr(G), kh(G) and khr(G) are foundation impedances which are functions of the dynamic shear modulus of the soil, G. The horizontal spring kx and rotational spring kk at the top of the column simulate the constraints imposed by the beams. The spring constants need to be calibrated using measured vibration properties. When the two ends of the Euler beam are fixed, the first natural frequency is calculated to be 283.85 Hz.

The modal frequencies and mode shapes extracted from vibration measurements are used to identify the physical parameters of the equivalent Euler beam and its spring constants. The identification process involves minimizing the following objective function [17]:

$$f(X) = \frac{1}{2}\left\| \begin{matrix} r_f(X) \\ r_s(X) \end{matrix} \right\|^2 \tag{12}$$

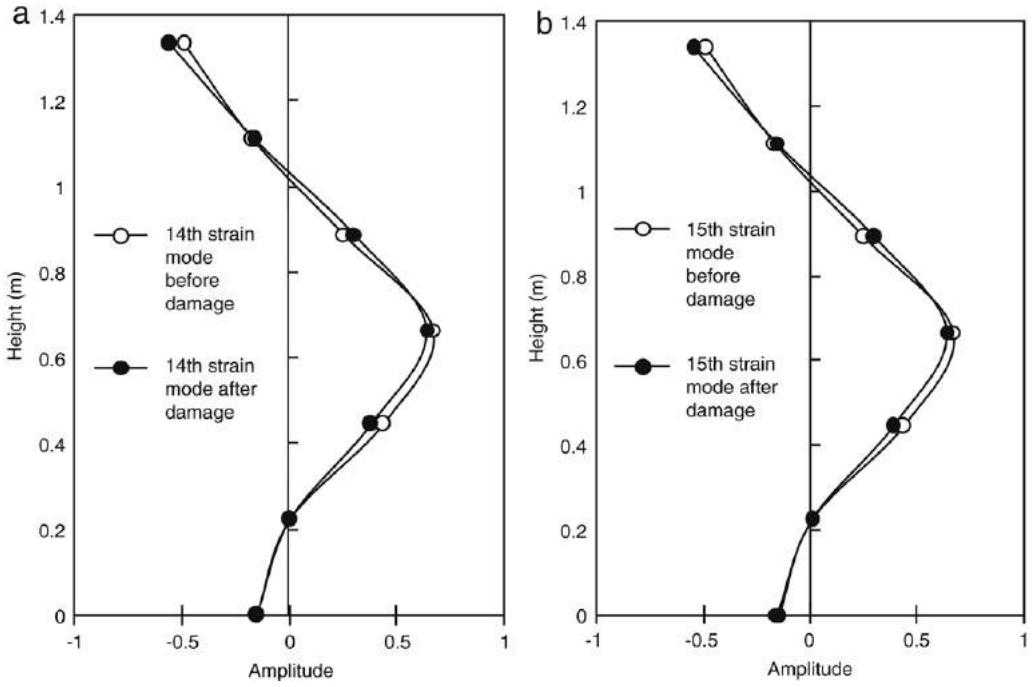

Fig. 17. Changes in strain mode shapes before and after damage; (a) 14th mode; (b) 15th mode.

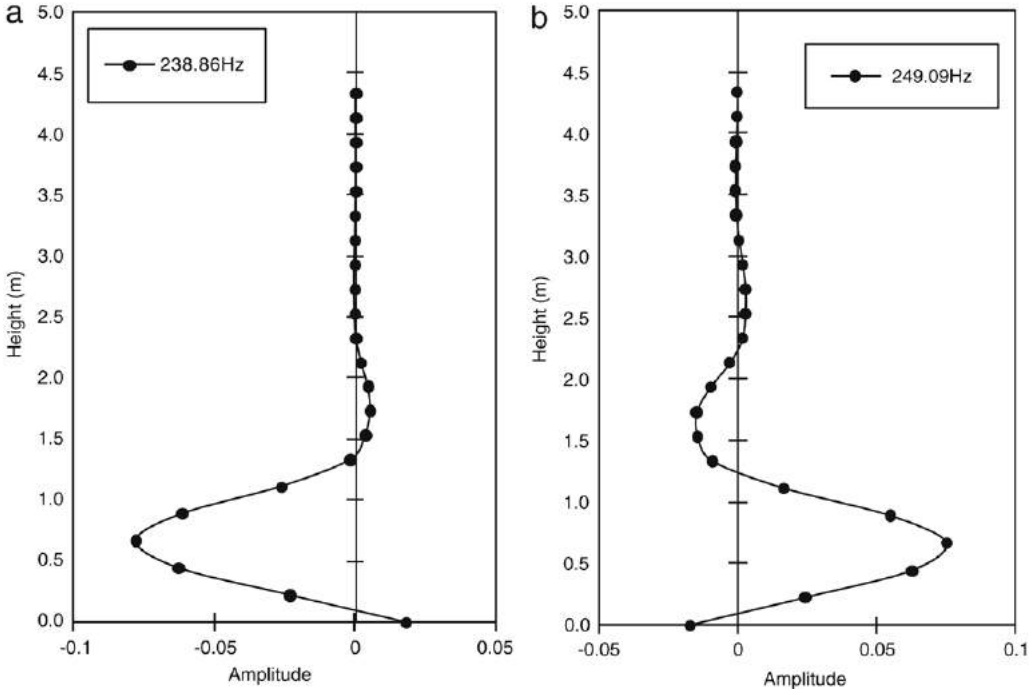

Fig. 18. Computationally simulated "highly sensitive higher modes" (HSHMs); (a) 5th mode; (b) 6th mode.

$$r_{f,i}(X) = \frac{\lambda_i(X) - \tilde{\lambda}_i}{\tilde{\lambda}_i} \quad \text{with } \lambda_i = (2\pi f_i)^2 \tag{13}$$

$$r_{s,i}(X) = \frac{\phi_i^l(X)}{\phi_i^r(X)} - \frac{\tilde{\phi}_i^l}{\tilde{\phi}_i^r} \tag{14}$$

In the above expressions, X contains the independent updating parameters, λ_i and ϕ_i = modal data obtained from the FE model, whereas $\tilde{\lambda}_i$ and $\tilde{\phi}_i$ are extracted from the measured data. The relative differences are used to obtain a similar weight for each frequency residual, r_f. The superscript r corresponds to the reference DOF to scale the mode shape, which is the one with the largest displacement and 'l' is any other DOF. The minimization is achieved through an optimal selection of the variable parameters $X = [E, G, kk, kx]$ that appear in the above equations. E is the elastic modulus of the column and G is the dynamic shear modulus under the isolated footing.

The 15th mode shape with natural frequency of 257.34 Hz is selected for the optimization of the four parameters G, E, kk and kx since this mode was the most sensitive to the added mass. The vibration shapes of the 7 points corresponding to the measurement points on the column are used. The identified parameters using

Table 10
Identified parameters using highly sensitive higher modes (HSHMs)

Identified parameter	E (N/m^2)	G (N/m^2)	kk (N/m^2)	kx (N/m)
Value	3.45×10^{10}	1.31×10^{8}	1.02×10^{9}	1.53×10^{9}

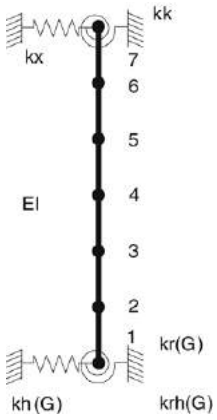

Fig. 19. Equivalent Euler beam model with two ends constrained by springs.

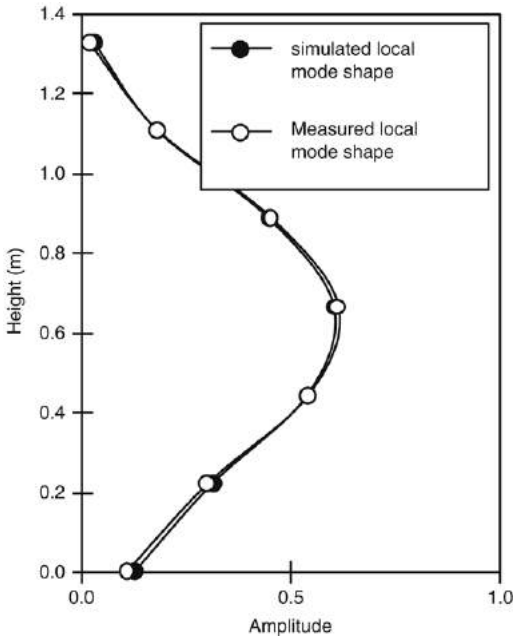

Fig. 20. Comparison of calculated and measured local mode.

the sensitivity analysis procedure described above are listed in Table 10 and the simulated mode shape is compared to the experimentally measured data in Fig. 20. The results of the identification process indicate that most of the parameters, with the exception of the shear modulus, compare well with the values in Table 2. The calculated HM using the constrained Euler beam model is 255.27 Hz, which compares reasonably well with the measured modal value.

5. Conclusions

Low level vibration testing consisting of hammer impact and sinusoidal sweeps using an electromagnetic oscillator were performed on a scale model four-story RC frame structure to identify both damage and physical parameters in a local member. Local damage was simulated by an added mass to a section of column on the lower floor of the frame. An advanced least-squares complex frequency-domain identification method 'PolyMAX' available in the LMS software [16] is used to analyze the frequency response functions of higher modes before and after simulated damage. The analytical and experimental results reported in this paper show that sensitive HMs can be used to identify localized damage and physical parameters. The following general conclusions are inferred from the study:

1. In real engineering structures, higher modes often exist in continuous beam-like structures and they can be found through experimental modal analysis by changing the physical conditions such as boundary conditions, support settlement, or changing the element mass or stiffness. HSHMs can be identified by introducing such changes, and the modes can be used in identifying physical parameters of local members in the system. The local mode shape of a continuous beam is known to be sensitive to the change in stiffness of the beam (other than a change in the length of the beam) in an equal span continuous beam, and the same is true for a column in a frame structure (even though the frame has equal story heights). Therefore, higher modes can also be used to judge whether the continuity of the continuous beam-like structure is broken.

2. The most significant sensitive higher modes for the four-story RC frame structure were identified. Seven distinct cases of local member variations were simulated using a simplified numerical model. A Diagnosing Index was defined to better identify changes in higher modes due to local damage. The length of the member and its end constraints were found to most significantly influence mode shape localization in HMs.

3. Higher modes characterize mode shape localization while LMs reflect global structural vibration modes. Localized mode shapes can be extracted from the frame's measured displacement and strain modes. The PolyMAX method [16] can be used to analyze the generated frequency response functions in order to identify distinct non-spurious vibration modes from which HMs can be recognized and analyzed.

4. HMs concentrate in several 'modal' regions of the FRF diagram called passbands. The order of the passband is identical to the order of the vibration mode shape of a single member's half sine wave.

5. Studies on the model frame with an added mass to simulate local damage indicate that selected HMs are sensitive to local changes and these modes are termed 'Highly Sensitive Higher Modes' (HSHMs). These modes concentrate in a small region and the magnitude of these modes are much larger than adjacent vibration shapes. HSHMs are found to be good candidates for local damage diagnosis.

6. The HSHMs in the present study were validated by numerical simulations. An equivalent Euler beam model with two ends constrained by translational and rotational springs is used to identify physical parameters of the local column and associated foundation. The analytically estimated parameters compare well with measured data.

Acknowledgements

Financial support provided by the National Natural Science Foundation of China (NSFC) under Grant No. 50678064 and the Fund for Science and Technology Plan Key Project by Hunan Province in PR China under Grant No. 06FJ3003.

References

[1] Cawley P, Adams PD. The location of detects in structures from measurements of natural frequencies. J Strain Anal 1979;14:49–57.
[2] Salawu OS. Detection of structural damage through changes in frequency: A review. Eng Struct 1997;19:718–23.
[3] Sohn H, Farrar CR, Hemez FM, Shunk DD, Stinemates DW, Nadler BR. A review of structural health monitoring literature. 1996–2001.
[4] Pierre C, Tang DM, Dowell EH. Localized vibrations of disordered multispan beams: Theory and experiment. AIAA 1987;25:1249–57.
[5] Bendiksen OO. Mode localization phenomena in large space structures. AIAA 1987;25:1241–8.
[6] Cornwell PJ, Bendiksen OO. Localization of vibrations in large space reflectors. AIAA 1989;27:219–26.
[7] Levne-West MB, Salama MA. Mode localization experiments on a ribbed antenna. AIAA 1993;31:649–69.
[8] Bouzit D, Pierre C. An experimental investigation of vibration localization in disordered multi-span beams. J Sound Vibration 1995;187:1565–77.
[9] Mester SS, Benaraga H. Localization in near periodic structures. AIAA 1994;4:1488–96.
[10] Cox AM, Agnes GS. A statistical analysis of space structure mode localization. AIAA 1999;4:3123–33.
[11] Shen H, Zhang RJ. Mode localization in transverse vibration of variable-density simply supported beam. Chinese Quart Mech 2004;25:118–23 [in Chinese].
[12] Xu L. Research on damage detection of reinforced concrete frame structures based on modal parameters. Ph.D. thesis. PR China: Hunan University; 2004 [in Chinese].
[13] Qi GZ, Guo X, Qi XZ, Dong W, Chang P. Local measurement for structural health monitoring. Earthq Eng Eng Vib 2005;4:165–72 [in Chinese].
[14] Wang XJ. Dynamic foundation and basement. Beijing: Science press; 2001 [in Chinese].
[15] Pais A, Kausel E. Approximate formulas for dynamic stiffness of rigid foundations. Soil Dyn Earthq Eng 1988;7:213–27.
[16] LMS International. LMS Test Lab – Structural Testing Rev 4B. Leuven. Belgium www.lmsintl.com 2003.
[17] Unger JF, Teughels A, Roeck GD. System identification and damage detection of a prestressed concrete beam. J Struct Eng 2006;132:1691–8.